Discovery of the Tomato Root Protein Network Exploited by Core Type 3 Effectors from the *Ralstonia solanacearum* Species Complex

Joren De Ryck[1,2,3,4], Veronique Jonckheere[3], Brigitte De Paepe[4], Annick De Keyser[1,2], Nemo Peeters[5], Johan Van Vaerenbergh[4], Jane Debode[4], Petra Van Damme[3*$] and Sofie Goormachtig[1,2*$]

[1]Department of Plant Biotechnology and Bioinformatics, Ghent University, 9052 Ghent, Belgium

[2]Center for Plant Systems Biology, VIB, 9052 Ghent, Belgium

[3]iRIP Unit, Laboratory of Microbiology, Department of Biochemistry and Microbiology, Ghent University, 9000 Ghent, Belgium

[4]Flanders Research Institute for Agriculture, Fisheries and Food, Plant Sciences Unit Burg. Van Gansberghelaan 96, 9820, Merelbeke, Belgium

[5]Laboratoire des Interactions Plantes Microorganismes Environnement (LIPME), INRAE, CNRS, Université de Toulouse, 31326, Castanet-Tolosan, France

* To whom correspondence should be addressed: Petra.VanDamme@UGent.be;

sofie.goormachtig@ugent.be;

[$] These authors share senior co-authorship

Running title: *Ralstonia* type III effector interactomics in tomato roots

ABSTRACT

Proteomics has become a powerful approach for the identification and characterization of type III effectors (T3Es). Members of the *Ralstonia solanacearum* species complex (RSSC) deploy T3Es to manipulate host cells and to promote root infection of, among others, a wide range of solanaceous plants such as tomato, potato and tobacco. Here, we used TurboID-mediated proximity labeling (PL) in tomato hairy root cultures to map the proxeomes of the core RSSC T3Es RipU, RipD and RipB. The RipU proxeome was enriched for multiple protein kinases revealing an impact on the two branches of the plant immune surveillance system, being the membrane-localized PAMP-triggered immunity (PTI) and the RIN4-dependent effector-triggered immunity (ETI) complexes. In agreement, a transcriptomics analysis in tomato revealed the potential involvement of RipU in modulating reactive oxygen species (ROS) signaling. The proxeome of RipB was enriched for mitochondrial and chloroplast proteins; that of RipD for proteins involved in the endomembrane system. Together, our results demonstrate that TurboID-PL in tomato hairy roots represents a promising tool to study *Ralstonia* T3E targets and functioning, and that it can unravel various host processes that can be hijacked by the bacterial pathogen.

KEYWORDS

TurboID, interactomics, plant immunity, proximity labeling, *Ralstonia solanacearum* species complex (RSSC), type III effectors (T3Es)

INTRODUCTION

Members of the *Ralstonia solanacearum* species complex (RSSC) are devastating phytopathogens threatening agriculture worldwide due to their broad host range and numerous survival and virulence strategies. Strains of RSSC are notorious agents of bacterial wilt disease in over 200 plant species, including various Solanaceous plants (e.g., potato, tomato, eggplant) and ornamental plants. This root pathogen colonizes and multiplies in the plant's vascular tissue, blocking upward sap flow and eventually resulting in wilting and death of the host plant and the subsequent release of the pathogen into the environment. An essential bacterial virulence determinant is the type III secretion system, pumping an array of virulence proteins (type III effectors, T3Es) into the host cell during infection. In total, over 100 different RSSC T3Es have been identified, with on average 46 to 71 T3Es per strain (https://iant.toulouse.inra.fr/bacteria/annotation/site/prj/T3Ev3/). Upon translocation to the host cell, T3Es collectively suppress the plant's immune response and establish host susceptibility. Several of these T3Es are common between strains, also referred to as 'core' effectors, possibly providing clues on the general infection strategies deployed by pathogens[1,2]. Core T3Es likely target conserved components of plant immunity and metabolism, and are therefore interesting breeding targets for durable resistance[3]. One example of such a core T3E is RipU, an effector that suppresses the reactive oxygen species (ROS) burst and induces mitogen-activated protein kinase (MAPK) expression upon ectopic expression in tobacco leaves[4]. Opposingly, less conserved T3Es could give insight into the respective strain's specific host adaption mechanisms.

Besides the recognition of microbial- or pathogen-associated molecular patterns (MAMPs/PAMPs), such as flagellin or the bacterial elongation factor Tu (EF-Tu), resulting in a MAMP/PAMP-triggered immunity (MTI/PTI) response, the plant's immune system has evolved to recognize some effectors or their activity by the deployment of plant resistance (R) proteins, often leading to a hypersensitivity response, a programmed death of invaded and surrounding cells,

preventing further spread of the pathogen inside the host[5]. In relation to *R. solanacearum*, the nucleotide-binding leucine-rich repeat (NB-LRR)-type *R* genes *RESISTANT TO PSEUDOMONAS SYRINGAE 4* (*RPS4*) and *RESISTANT TO R. SOLANACEARUM 1* (*RRS1*) from *Arabidopsis* (Brassicaceae) recognize the T3E RipP2 (also known as PopP2), leading to resistance, and expression of these *R* genes in tomato (*Solanum lycopersicum*) similarly results in the resistance against *R. solanacearum*[6].

Recognition by R proteins often happens indirectly via the "guard" model in which many R proteins survey the status of a guardee, the plant effector target[7]. One of the most studied guardees is the *Arabidopsis* protein RPM1-INTERACTING PROTEIN 4 (RIN4), whose modification by effectors is monitored by, for instance, the R proteins RESISTANT TO *P. SYRINGAE* 2 (RPS2) and RESISTANCE TO *P. SYRINGAE* PV MACULICOLA 1 (RPM1)[8-10]. RIN4 is localized at the plasma membrane (PM) with multifunctional roles in both the PTI and ETI. Besides its role in the activation of ETI, depending on its phosphorylation status, it can exert a positive or negative role in PTI and additionally controls stomatal closure upon PAMP perception by interacting with two PM H^+-ATPases AHA1 and AHA2[11-13]. The RIN4 immune complex is therefore a target of particular choice for modulation by T3Es. Indeed, several *P. syringae* T3Es (AvrB and AvrRpm1) impact the phosphorylation status of RIN4 through host kinases to suppress the basal defense and closing of stomata, thereby promoting invasion of the leaf pathogen[14,15]. Other T3Es (AvrPto, AvrPtoB, AvrRpt2, HopPtoQ1-1 and HopAM1) also modulate RIN4 degradation and thus RIN4 activity, which is sensed by the RPS2 guard protein[16]. Upstream targets of RIN4 can also be modified by T3Es, thereby modulating RIN4 activity, as exemplified by the *P. syringae* T3E HopZ3 acetylating the tomato RIN4-interacting receptor-like protein kinase SlRIPK, resulting in the suppression of its kinase activity and phosphorylation of its SlRIN4 target[17]. Besides the RIN4 pathway, many other signaling cascades are shared between plant species and control the interplay between the PTI and ETI response. Examples are members of the MAPK pathways such as MPK3/6 in Arabidopsis[18].

Information on plant immunity largely stems from research performed in shoot tissue, and our understanding of root immunity, and concomitantly the infection strategy of root pathogens, is therefore severely limited[19]. Although many RSSC T3Es have a known involvement in virulence or ETI triggering, based on the results from virulence assays (e.g., ROS, callose deposition and hypersensitivity response induction assays, mainly performed in tobacco leaves), very little is known about their exact *in planta* function[20].

Screening for protein–protein interactions (PPIs) might provide additional clues on effector functions. To date, the most commonly used high-throughput screening technologies to identify novel plant PPIs are yeast two-hybrid library screening coupled to next-generation sequencing (Y2H-seq), and mass spectrometry (MS)-based proteomics methods such as affinity purification (AP)-/ immunoprecipitation (IP)-MS and enzyme-catalyzed proximity labeling (PL-MS)[21-24]. In a large-scale Y2H-seq experiment, the *R. pseudosolanacearum* strain GMI1000 and *Xanthomonas campestris, pv campestris* strain 8004 were matched with Arabidopsis proteins, resulting in a large interactomics network available at https://lipm-browsers.toulouse.inra.fr/k/EffectorK/[25]. IP-MS experiments were, for example, performed for the RSSC T3Es RipAB, RipAC, RipAK, RipAY and RipI to screen for plant protein interactors[26-30]. Compared to AP-MS and Y2H-seq, which are mainly used for the discovery of direct protein interaction partners, enzyme-catalyzed PL identifies proximal protein targets (jointly referred to as the proxeome). In this case, the protein of interest, also referred to as bait protein, is tagged with a (modified) enzyme capable of covalently modifying bait-proximal proteins. PL can be used for the identification of membrane proteins and has the advantage of labeling proteins in intact cells or tissues, allowing physiologically relevant protein interactions to be captured even when weak or transient. Enzyme-catalyzed PL uses promiscuous mutant biotin ligase (such as TurboID and miniTurboID) fused to the bait protein of interest to biotinylate proximate and interacting proteins, after which these interactors can be purified with streptavidin-coated beads and identified via MS. TurboID and miniTurbo have successfully been

applied in various plant species and models (e.g., *Arabidopsis thaliana*, *Nicotiana benthamiana* and *S. lycopersicum* hairy root cultures) for the identification of known and novel plant protein interactors and the mapping of plant protein signaling networks[31-36].

Here, we mapped the proxeomes of several core T3Es from the RSSC to investigate their mode of action in tomato roots. The proxeome of RipU in particular revealed multiple protein kinase targets, of which many Arabidopsis homologs are known to be located in the RIN4-containing microdomain at the PM, adding in-depth insight into how this effector controls immunity when expressed in tomato roots.

MATERIALS AND METHODS

TurboID-MS Analysis in Tomato Hairy Root Cultures

Plant Materials and Growth Conditions

Tomato (*S. lycopersicum* cv Moneymaker) seed surfaces were sterilized with 3% sodium hypochlorite solution. The seeds were washed three times with sterile water and placed onto solid Murashige & Skoog (MS) medium containing 4.3 g/L MS (Duchefa, The Netherlands; catalog no. M0221.0050) and 0.5 g/L MES (Duchefa; catalog no. M1503.0100). The pH was set to 5.8 with KOH and 10 g/L plant agar (BD Difco™, France; catalog No. 214530) was added before autoclaving for 20 min at 121°C. After 2 days of vernalization in the dark at 4°C, the plates were transferred to a growth chamber under a 16-h/8-h light/darkness photoperiod at 24°C for 7 to 10 days. Fully expanded cotyledons were cut and used for hairy root transformation. Resulting tomato hairy roots were grown in the dark at 24°C on solid or in liquid MS medium containing 3% sucrose (3% MS).

Bacterial Strains and Cloning of Constructs

Escherichia coli (*E. coli*) strain DH5α was used for standard transformation protocols. Electrocompetent *Agrobacterium rhizogenes* (*A. rhizogenes*) strain ATCC15834[37] was used for hairy root transformation. The full-length open reading frame (ORF) sequence of the *Ralstonia pseudosolanacearum* GMI1000 (Rps GMI1000) T3E *RipB* was cloned into the pDONR207 vector, and the ORFs of *RipH1* and *RipH3* were codon-optimized for *in planta* expression and cloned into the pUC57 vector. Genomic DNA was purified from a Rps GMI1000 culture using the Maxwell® RSC Cultured Cells DNA Kit and the Maxwell® RSC 48 Instrument, following the manufacturer's instructions. The *RipAJ*, *RipD* and *RipU* sequences were PCR-amplified from the genomic DNA using high-fidelity iProof DNA polymerase and primers containing (Gateway-cloning compatible) *attB* recombination sequences (**Table S1**). Resultant *attB*-flanked PCR products were used in a Gateway BP recombination reaction with the pDONR221 vector (Life Technologies, Carlsbad, CA, USA) according to the manufacturer's instructions, thereby creating an entry clone. The entry constructs were transformed in DH5α and verified by Sanger sequencing. Using a standard multisite (3-fragment) Gateway LR cloning strategy as described in Van Leene, et al.[38] , the entry clones together with the pEN_L4R1_RPS5α_XVE entry clone encoding the β-estradiol-inducible *XVE* promoter[39], and pEN_R2L3_GGGGS_Turbo_FLAG (PSB database vector ID 12_30) encoding the Flag-tagged TurboID, were recombined into the pKCTAP destination vector (PSB database vector ID 2_18)[38] to generate expression constructs encoding translational fusion between the baits (GFP, RipAJ, RipB, RipD, RipH1, RipH3 or RipU) and the TurboID-Flag tag[31] under control of the *XVE* promoter. The pKCTAP destination vector allows selection of transformed roots by expression of GFP driven by the *rolD* promoter and a kanamycin resistance gene sequence between the left and right border of the root-inducing (Ri)- DNA from *A. rhizogenes*.

Tomato Hairy Root Transformation, Cultivation and Collection

Tomato hairy root cultures were generated as described in Arora, et al.[31] . In short, fully expanded cotyledons were cut, inoculated with transformed *A. rhizogenes* ATCC15834 harboring the expression vector (OD at 600 nm of 0.3) and placed onto a cell culture dish containing solid 3% MS medium (abaxial side facing up). After three days of co-cultivation in the dark, the cotyledon explants were transferred to a new cell culture dish containing 3% MS with 200 µg/mL cefotaxime (Duchefa; catalog no. c0111.0025) and 50 µg/mL kanamycin (Duchefa; product code K0126). After 2 to 3 weeks, 4 to 10 independent roots emerging from the cotyledons were selected for *GFP* expression (using a Leica stereomicroscope with ET GFP long pass filter) and transferred to a new cell culture dish containing 3% MS with antibiotics for three rounds of subculturing, after which they were maintained on 3% MS medium without antibiotics. Branched hairy root culture (covering ~4 cm^2 of surface) were transferred to 50-mL Falcon tubes containing 10 to 30 mL of liquid 3% MS medium sealed with AeroPore tape (Aero Healthcare), and grown for 2 to 3 weeks in the dark at 24°C on a tabletop shaker at 150 rpm. After 2 to 3 weeks of growth in liquid culture, expression of the *bait-TurboID-Flag* construct was induced with 100 µM of 17β-Estradiol (Sigma-Aldrich, product code D8418) and after 22 h, 50 µM of biotin was added to the hairy root liquid culture, which was grown for an extra 2 h on the tabletop shaker.

TurboID-Mediated PL

Four independent hairy root clones with validated protein expression as observed by immunoblotting were selected per bait. TurboID-mediated PL involves protein extraction from tomato hairy root cultures, followed by proximity biotinylation, proteomics sample preparation, immunoblot analysis quality control and LC-MS/MS analysis, essentially as reported in Gryffroy, et al.[33] and described in detail in **Supporting Materials and Methods**.

Shotgun Proteome Analysis

Crushed root material obtained for proximity biotinylation was also used for shotgun proteome analysis. Here, three independent hairy root clones with validated protein expression as observed by immunoblotting were selected per bait. Shotgun proteome analysis involves protein extraction, followed by proteomics sample preparation and LC-MS/MS analysis, described in detail in **Supporting Materials and Methods**.

Gene Expression Analysis

Crushed root material expressing GFP-TurboID or RipU-TurboID obtained for proximity biotinylation was also used for gene expression analysis. Total RNA was extracted from 100 mg of ground tomato hairy root cultures from three independent biological repeats using the Reliaprep™ RNA Miniprep System (Promega, Madison, WI, USA) following the manufacturer's instructions. Quality and concentration of the RNA was checked using the NanoDrop™ One/One^{C} Microvolume UV-VIS spectrophotometer (Thermo Scientific™, Waltham, MA, USA). Total RNA was sent to BGI Genomics (Hong Kong) for transcriptomic analysis (DNBSeq-G400; 20 M reads/4 Gb per sample; 100-bp single-end reads). Reads were mapped to the *S. lycopersicum* Exome ITAG4.0 using the Salmon mapping tool[40] and statistical analysis was done in R with the edgeR package. Models of expression contrasts were fitted with a generalized linear regression model and fitted values of the three biological replicates were grouped per setup. Lowly expressed genes (logCPM < 1.5) were filtered out and significantly differentially expressed genes were retrieved by the following criteria: logCPM ≥ 1.5,|logFC| > 3, p-value ≤ 0.01 and FDR ≤ 0.01. Gene ontology (GO) enrichment analysis was performed using PLAZA 5.0 Dicots[41].

Real-Time Quantitative Reverse Transcription PCR (RT-qPCR)

1 µg of total RNA was converted into cDNA using the qScript cDNA synthesis kit (Quantabio, Beverly, MA, USA), following the manufacturer's instructions. The cDNA was finally diluted to

500 µL using nuclease-free water, obtaining a final concentration of 2 µg/mL. RT-qPCR analyses were performed for three technical replicates per sample using the Fast SYBR Green Master Mix (Applied Biosystems, Waltham, MA, USA) with a final concentration of 0.25 µM for each primer. The Roche Lightcycler 480 system (Roche Diagnostics, Switzerland) was used to execute all RT-qPCR reactions. *S. lycopersicum* transcript abundance was normalized using the housekeeping genes *SlACT* (*Solyc03g078400*), *SlGAPDH* (*Solyc05g014470*) and *SlTUB* (*Solyc04g081490*). The primers used for RT-qPCR are listed in **Table S1**. After normalization, relative fold changes were calculated using the delta-delta Ct method ($2^{\Delta\Delta Ct}$) and results were analyzed in qBase+.

Co-Localization in Tomato Hairy Root Lines

For subcellular localizations in tomato hairy root lines, mCherry was C-terminally fused to *RipU* under the control of the constitutive *CaMV35S* promoter and cloned into the pGGIB-U2-A-ccdBCmR-G-U3 destination vector by Gibson assembly. Prey sequences were C-terminally fused to GFP under the control of the *pUBI* constitutive promoter and cloned into the pGGIB-U1-A-ccdBCmR-G-U2 destination vector. *RipU-linker-mCherry* and *prey-linker-GFP* vectors were assembled into one destination vector using the vectors pGGIB-U3-L3-U9 and pK-U1-A-ccdB-G-U9 to yield pK-pUBI-prey-link-GFP-G7T-p35S-RipU-link-mCherry-35ST (primer sequences are listed in **Table S1**). Constructs were transformed into *E. coli* DH5a and integrity of the construct was checked by Sanger sequencing. The vectors were obtained by GeneJET plasmid DNA Miniprep (Thermo Scientific) following the manufacturer's instructions and subsequently transformed into *A. rhizogenes* strain ATCC15834. Tomato hairy root cultures expressing the construct were created as described above, and expression of RipU-mCherry and prey-GFP was confirmed by fluorescence microscopy.

For subcellular co-localization analysis in *N. benthamiana* leaves and tomato hairy root lines, GFP and mCherry were imaged using the Zeiss inverted LSM710 confocal laser microscope, equipped with objective Plan-Apochromat 20x/0.8 M27. The 488-nm and 587-nm lasers were used

for excitation of GFP and mCherry, respectively, and GFP and mCherry fluorescence were detected using a 505- to 530-nm bandpass emission filter and 610-nm long pass filter, respectively.

RESULTS

TurboID-Mediated Proximity Labeling of Core Ralstonia T3Es

We made use of the recently established platform for TurboID-mediated PL in tomato hairy roots[31,33] to identify plant protein interactors of six core T3Es from the RSSC. The Rps GMI1000 T3Es RipAJ, RipB, RipD, RipH1, RipH3 and RipU together with the control, green fluorescent protein (GFP), were C-terminally fused to Flag-tagged TurboID (from here on referred to as 'TurboID') under the control of a β-estradiol-inducible promoter (*XVE*). These effector baits were selected based on their identification as core effectors, which might have conserved protein targets in various plant hosts[1,2], and the fact that they are under positive selection, have an unknown function, and have a reported involvement in tomato pathogenicity (i.e., RipH1, RipH2, RipH3 and RipU)[1,42,43], as well an observed expression in tomato hairy root cultures. Inducible effector- or control (GFP)-TurboID-expressing tomato hairy root cultures were obtained by *A. rhizogenes*-mediated transformation and hairy root cultures were induced for 24 h with β-estradiol and 50 µM biotin was added 2 h prior to root collection, protein extraction and TurboID-MS sample preparation (see Materials and Methods). The total proteome extracts of four independent hairy root clones per bait were then subjected to immunoblot analysis to examine bait integrity (using the α-FLAG antibody targeting the (T3E-)TurboID-FLAG fusion protein) and cis- and trans-biotinylation activity of the fusion protein (using the streptavidin/Alexa Fluor™ conjugate) (**Figure S1**). When probing for biotinylation using a streptavidin conjugate, trans-biotinylation could be detected in all setups. Observable (cis)-biotinylation could however only be detected for the GFP-, RipAJ-, RipB-, RipH3- and RipU-TurboID fusions. The endogenously biotinylated proteins acetyl-

CoA carboxylase 1 and 2 (ACC1 and ACC2, 70/75 kDa, respectively) could also be detected (**Figure S1**).

During the TurboID-MS sample preparation, prior to MS analysis, equivalent fractions were obtained (total lysate, desalted lysate and streptavidin-unbound lysate) and analyzed alongside the streptavidin-bound fraction obtained to assess the efficiency of the isolation of biotinylated material and the overall quality of the TurboID protocol (**Figure 1**).

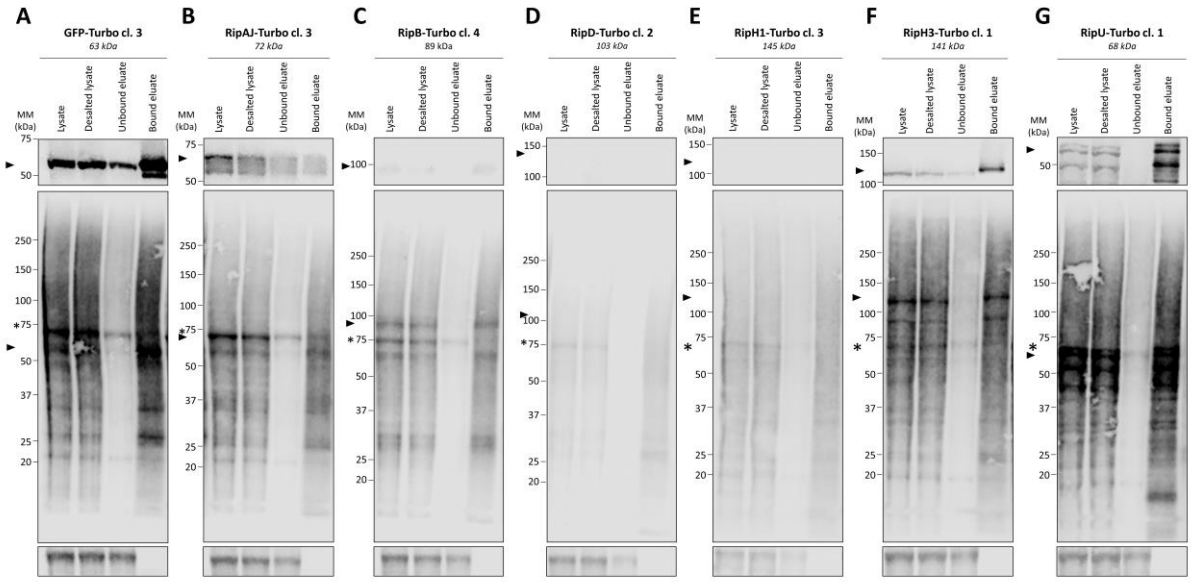

Figure 1. Immunoblot analysis of samples taken during the TurboID-MS sample preparation. Prior to subjecting TurboID samples to MS, a quality assessment of the sample preparation of one representative biological replicate (GFP-TurboID (A), RipAJ-TurboID (B), RipB-TurboID (C), RipD-TurboID (D), RipH1-TurboID (E), RipH3-TurboID (F) and RipU-TurboID (G)) was performed by subjecting the input tomato hairy root protein lysate, desalted, unbound and bound lysate fractions collected at various steps of the procedure to immunoblot analysis. Immunoblotting was performed to probe for expression of the bait-TurboID fusion protein (α-FLAG antibody, upper panel), biotinylated proteins (streptavidin/Alexa Fluor™ 680 conjugate, middle panel) and a loading control (α-ACT8 antibody, bottom panel). Arrows indicate the size of the fusion proteins and the asterisks indicate the band corresponding to the endogenously biotinylated proteins acetyl-CoA carboxylase 1 (ACC1) and ACC2. MM indicates the protein molecular weight marker.

Biotinylated proteins were efficiently captured in the bound fraction (comparing bound and unbound fractions) during overnight incubation with streptavidin-coated beads. This is also evident from the absence of the non-biotinylated ACT8 protein in the bound fraction (**Figure 1, lower panels**). Although the protein expression levels of RipB-, RipD- and RipH1-TurboID appeared relatively low, the biotinylation signal corresponding to the respective bait fusions was still evident in the bound eluates (**Figure 1; C, D, E**). Together, the immunoblot analyses confirmed effective isolation of biotinylated material from tomato hairy roots expressing GFP-TurboID or T3E-TurboID.

Following on-bead tryptic digestion, tryptic peptides were analyzed by LC-MS/MS for protein identification and quantification. To enable relative interactome comparisons, we performed label-free quantification (LFQ) on four biological replicate samples per bait using the MaxLFQ algorithm[44]. Retained replicate samples (minimum 3, based on initial data quality inspection) indicated a good (Pearson) correlation of replicate samples while showing a higher variability with the other bait setups (**Figure 2, A**).

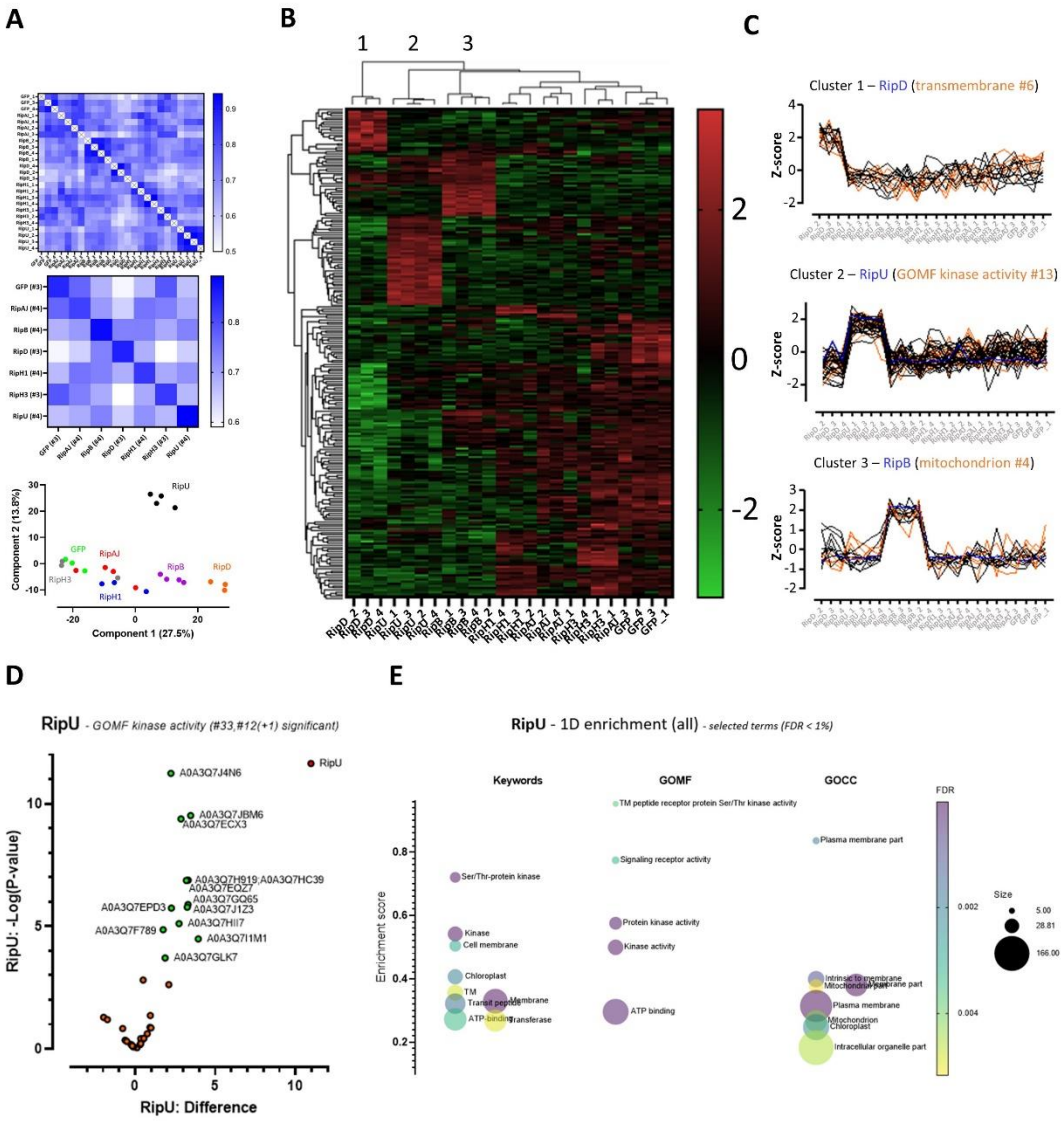

Figure 2. Proximity-dependent biotin identification (TurboID) enables the discovery of differential *Ralstonia* effector interactors. (A) Heat map visualizations of pairwise LFQ correlations (Pearson) for all replicate samples considered (top) and averaged per setup across replicates (middle), PCA plot of the variability between the different setups and replicate TurboID samples analyzed (bottom). Green, red, blue, gray, purple, black and orange indicate GFP, RipAJ, RipH1, RipH3, RipB, RipU and RipD setups, respectively. (B) Heat map representation of cluster analysis after ANOVA. The imputed intensities of proteins with significantly different abundances (FDR ≤ 0.01) in the respective proxeomes (#231 protein entries) are represented. Three clusters (clusters 1-3), respectively enriched for RipD, RipU and RipB interactors can be observed. Green and indicate low and high intensities, respectively. Volcano plot representations of the data can be found in **Figure 2D** (RipU) and in **Figure S2** (other baits). (C) Profile plots of enriched GO terms with significant increased abundances (FDR ≤ 0.05) are shown for

the three indicated clusters across all replicate samples and setups analyzed. GOMF = GO-term Molecular Function. Results from three to four independent hairy root clones per bait induced with 100 µM β-estradiol for 24 h and supplemented with 50 µM biotin 2 h prior to analysis. (D) t-Test results (#618 protein entries) of RipU versus complement, filtered for proteins with corresponding GOMF term 'kinase activity' (#33 entries) are visualized in a volcano plot. Significant enriched data points indicated in green are based on a permutation-based FDR calculation as compared to the complement. The pairwise t-tests were performed with an FDR of 0.01 and S0 of 0.1. The RipU bait identified is indicated in red. Volcano plot representations of the data for the other baits can be found in **Figure S2**. (E) Multiple variable bubble plot representations of significantly enriched GO terms for the RipU setup. Enriched GO terms (GOMF, GO-term Cellular Component (GOCC) and keywords) ($P \leq 0.01$) are shown. Term enrichment was determined using 1D annotation enrichment[45] based on annotation of *A. thaliana* homologs and p values were corrected for multiple hypotheses testing using the Benjamini and Hochberg FDR. Only representative/selective non-redundant terms with at least five members and corrected p values < 0.01 were considered. The bubble size corresponds to the number of regulated proteins with a given GO term and the color code represents the FDR scale. The full list of 1D enriched GO terms can be found in **Table S3**.

Reference groups were defined as the complement group of each setup (i.e., the union of all other setups)[46] and subjected to a pairwise t-testing (**Figure S2**) (**Table S2, S2b**). All baits were found to be significantly enriched in their respective bait-TurboID setups analyzed. Only few or no significantly enriched proximal proteins (FDR 0.01) could be detected for RipAJ-Turbo, RipH1-Turbo and RipH3-Turbo (1, 0 or 2, respectively); with the alkaline/neutral invertase (A0A3Q7GBX5) enriched for RipAJ ($P \leq 0.01$, 8 unique peptides, 24.6% sequence coverage), no significant targets for RipH1, and the NB-LRR Arabidopsis homologs RECOGNITION OF PERONOSPORA PARASITICA (RPP8)-like protein (A0A3Q7G0L5, 11 unique peptides, 11.6% sequence coverage) and CLIP-associating protein 1 (CLASP1)-like protein (A0A3Q7I3D7, 21 unique peptides, 21.5% sequence coverage) in case of RipH3. More significantly enriched proteins could be detected for the RipB, RipD and RipU baits (**Table S2**).

To reveal (differential) effector proximal proteins (FDR ≤ 0.01), we grouped and compared replicate and reference samples by multiple ANOVA testing. The intensities of significant differential interactors are shown as heat maps after z-score transformation and non-supervised hierarchical row clustering (multiple ANOVA testing) (**Figure 2, B, Table S5**). ANOVA analysis revealed three clusters (clusters 1-3), respectively enriched for RipD, RipU and RipB proximal proteins. Due to a rather poor GO annotation of *S. lycopersicum*, we used *A. thaliana* homologs annotation for GO enrichment analysis[45]. A 1D annotation enrichment analysis revealed among other enriched terms (**Table S3**) the enrichment of transmembrane (helix) (RipD, keywords), mitochondrion (RipB, keywords), and kinase activity (RipU, GO Molecular function), respectively (**Figure 2, C**).

Besides the enrichment of mitochondrial proteins, several chloroplast proteins were also found enriched in case of RipB, as well as two cystathione β-synthase (CBS)-domain containing proteins (A0A3Q7JUM6 and A0A3Q7J7U0), whereas putative RipD interactors included many proteins involved in vesicle trafficking, the endomembrane system and intracellular protein transport (**Table S2**). Interestingly, 42% (14/33) of the enriched RipU interactors were annotated as (receptor) (Ser/Thr) kinase proteins (**Figure 2; D, E**), a finding that, to our knowledge, has not yet been reported to this extent for any other bacterial effector.

In addition, the GO-term 'plasma membrane' is overrepresented in the RipU interactor dataset (**Table S3**). One example of an enriched PM-localized receptor-like kinase is FERONIA, a PAMP receptor involved in powdery mildew infection and H^+-ATPase 2 (AHA2) accumulation under dim-light growth conditions[47-49], and activation of the MAPK pathway upon recognition of the secreted virulence protein from *Botrytis cinerea* endopolygalacturonase 1 (BcPG1)[50]. Next to Ser/Thr- and Pto-like kinase proteins, some proton transporters (AHA11 and AHA2) (**Figure S3**) and remorin proteins (REMORIN1) – essential regulators of plant defense[51] – were enriched in the RipU samples, as well as RESISTANCE TO P. SYRINGAE PV MACULICOLA 1- INTERACTING PROTEIN 4

(RIN4) homologs (**Figure S4**) and the RESPIRATORY BURST OXIDASE HOMOLOG B (RBOHB) protein (**Figure S5**, **Table S2**). Finally, the CC-NBS-LRR Resistance protein (K4BDY9) and Plant Intracellular Ras-group-related LRR protein 4 (PIRL4) homologs were also found enriched in the RipU proxeome (**Figure S5**, **Table S2**). Overall, these findings suggest that RipU functions at the PM with a potential involvement in the modulation of PTI/ETI signaling.

To complement the TurboID-MS data and look at possible proteome-wide expression changes upon effector expression, three matching biological repeats per bait-TurboID setup were subjected to shotgun proteomics. Notably, no significant differences, aside from the upregulated bait sequences, were observed compared to the complement in a pairwise t-test performed with an FDR of 0.01 and an S0 of 0.1 (**Figure S6**). Only for RipH3, the PDZ domain-containing protein A0A3Q7FAG8 was significantly downregulated (7-fold). The PDZ domain was first identified in the postsynaptic density protein 95 (PSD-95), the septate junction protein discs-large in Drosophila, and the epithelial tight junction protein zonula occludens-1 (ZO-1) and is likely involved in PPI to regulate subcellular localization[52]. Thus, generally, no significant steady-state protein expression changes were evident 24 h after induction of the T3E-bait fusion protein, hence differences in protein expression do not account for the different effector bait proximal partners here identified by TurboID-MS.

Together, these results demonstrate the potential of TurboID-MS in selectively identifying proximal protein partners and hint on different subcellular host localization and functioning of *Ralstonia* T3Es in tomato hairy root cultures, with an enriched group of proximal mitochondrial proteins, vesicle trafficking proteins and kinases, as well as other PM-associated proteins for RipB, RipD and RipU, respectively.

In-Depth Characterization of the RipU Proxeome

Intrigued by the unique identification of a large number of kinases in combination with proteins known to be involved in PTI and ETI, we tested whether RipU and its putative proximal targets, as

identified by TurboID-MS, localize to the same subcellular compartment. Therefore, we co-expressed RipU and the tomato RIN4.1 (SlRIN4.1) in tomato hairy root cultures. In addition, we also co-expressed RipU with the protein kinase domain-containing protein (accession A0A3Q7JBM6) that was highly enriched in the RipU proxeome, either as full-length (FL) or its corresponding kinase domain. For this, RipU was C-terminally fused to mCherry and expressed under the control of the constitutive *CaMV35S* promotor, while RIN4.1 and A0A3Q7JBM6 (FL or kinase domain) were C-terminally fused to GFP and expressed under the control of the constitutive *UBI* promotor (**Figure 3**). Both fusion proteins were expressed from the same Ri-DNA (see Materials and Methods).

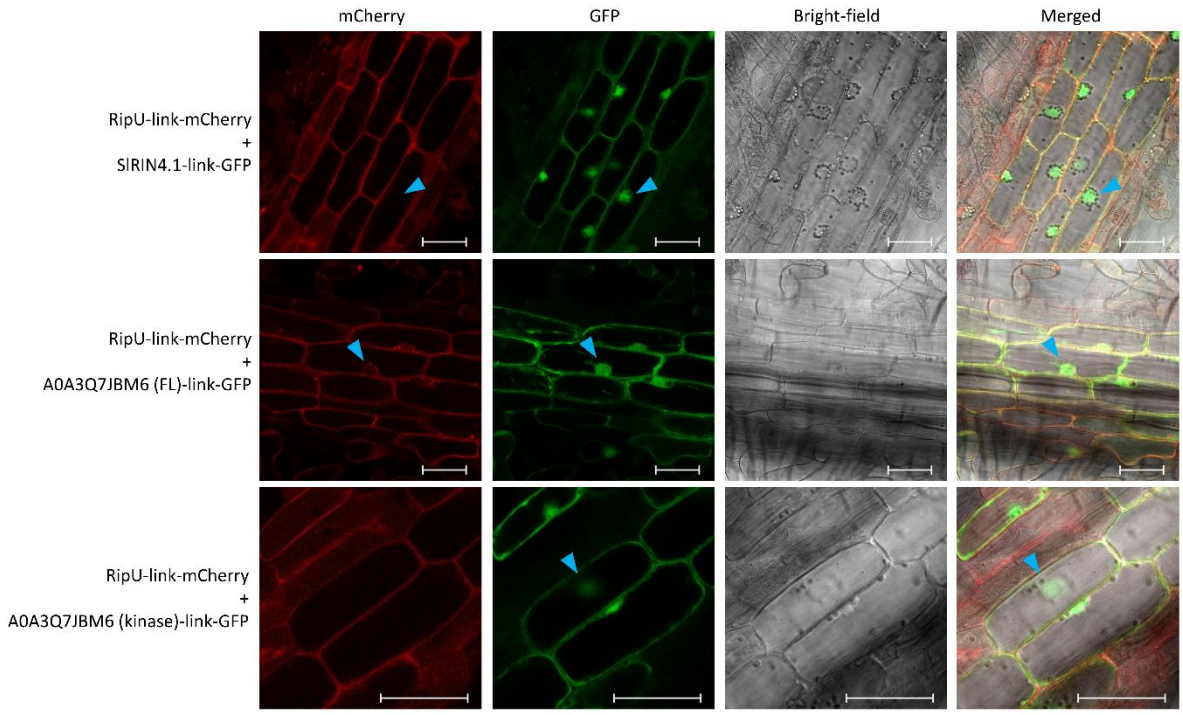

Figure 3. RipU co-localizes with RIN4.1, full-length (FL) A0A3Q7JBM6 and A0A3Q7JBM6 kinase domain in the cell periphery of tomato hairy root cells. Subcellular localization of RipU, RIN4.1 (Solyc06g083390), FL A0A3Q7JBM6 (protein kinase, Solyc12g062280) and the kinase domain of A0A3Q7JBM6 in tomato hairy root cultures. RipU was C-terminally fused to mCherry and expressed under the constitutive *CaMV35S* promotor, while RIN4.1 and A0A3Q7JBM6 (FL and kinase domain) were C-terminally fused to GFP under the control of the constitutive *UBI*

promotor. Both fusion proteins were expressed from the same Ri-plasmid. Left panel: mCherry fluorescence, second panel: GFP fluorescence, third panel: bright-field, right panel: overlay of all channels. Representative pictures from three independent biological repeats. Blue arrowheads indicate a nucleus. Scale bars = 50 µm.

In tomato root cells, RipU was found to mainly localize in the cytoplasm (**Figure 3, arrow**). The RipU preys RIN4.1 and A0A3Q7JBM6 (FL or kinase domain) seem to co-localize in the cytoplasm, but were additionally clearly localized in the nucleus of tomato hairy root cells. Similar results were obtained by tobacco infiltration (**Figure S7**). In addition to cytoplasmic localization, RipU was observed in the nucleus of tobacco leaf cells (**Figure S7**). Together, these results show co-localization of RipU with its proximal proteins RIN4.1 and A0A3Q7JBM6 (FL or kinase domain) in tomato hairy root cells.

Since the RipU proxeome let us hypothesize that RipU interferes with the plant immune system, we further assessed RipU functioning by analysis of putative transcriptional changes upon *RipU* expression in tomato hairy root cultures using RNA-sequencing (RNA-seq). RNA-seq was performed on total RNA extracted from three independent hairy root clones expressing either *GFP-TurboID* or *RipU-TurboID*. Fifteen differentially expressed genes, of which two were downregulated and thirteen upregulated, were identified when considering $|\log FC| > 3$, FDR < 0.05 and logCPM > 1.5 (**Table S4**). When performing GO enrichment analysis, a significant enrichment in GO terms related to oxidative stress (hydrogen peroxide catabolic process, peroxidase activity, response to chemical) was observed in the set of upregulated genes, among which several peroxidases and cell wall-modifying enzymes (**Figure 4, A**).

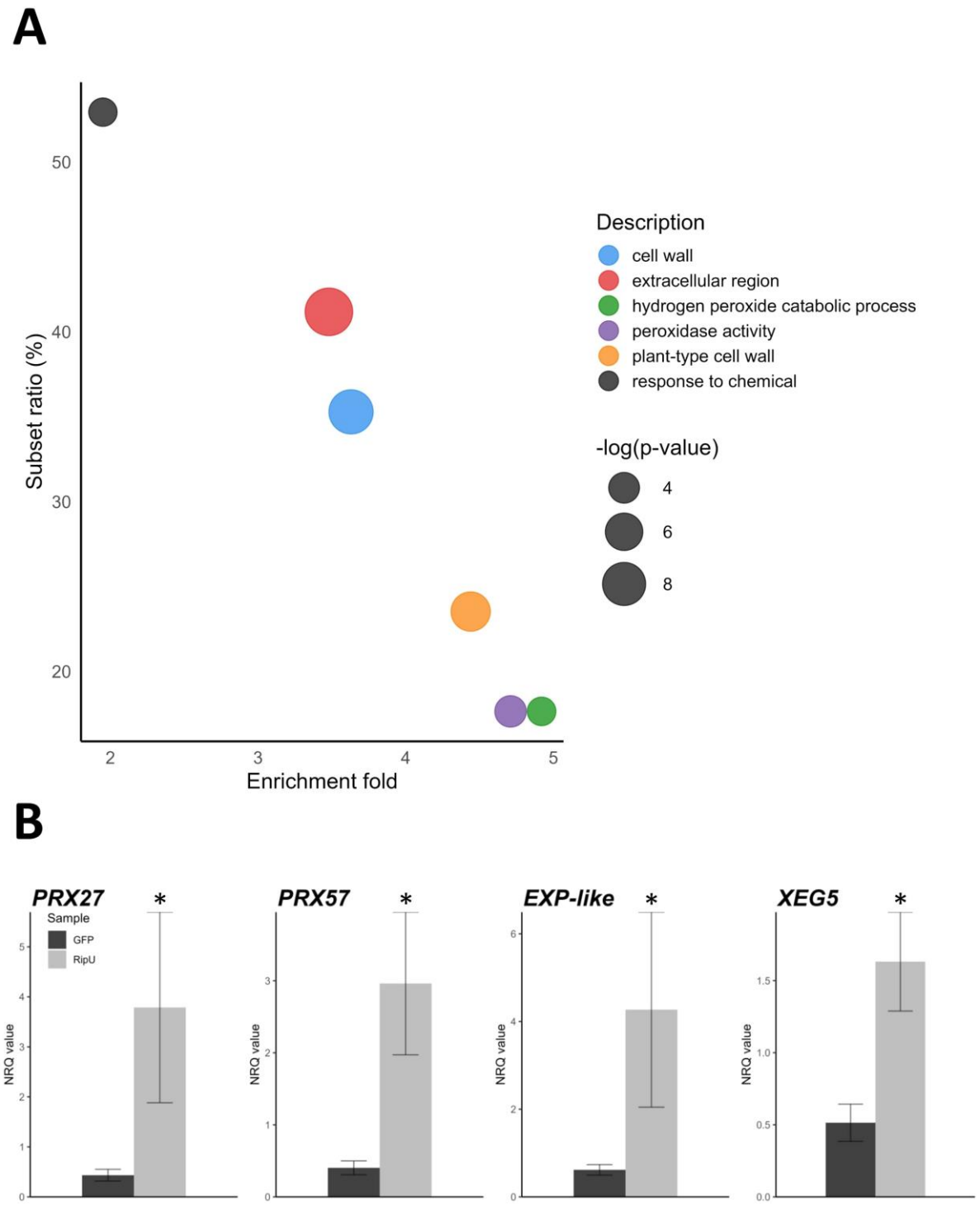

Figure 4. *RipU* expression results in changes in oxidative stress-related gene expression in tomato. (A) Differentially expressed genes were identified by means of RNA-seq between tomato hairy root cultures expressing either *GFP-TurboID* or *RipU-TurboID* using the criteria |logFC| > 3, FDR < 0.05 and logCPM > 1.5. A GO enrichment analysis was performed on the upregulated genes (#13) and downregulated genes (#2) compared to the GFP samples. The GO terms are represented in **Table S3**. (B) An RT-qPCR was performed on tomato hairy root

samples either expressing *GFP-TurboID* or *RipU-TurboID* using primers targeting different enriched genes as determined by RNA-seq. *PRX* = *Peroxidase* (*Solyc08g075830*, *Solyc01g009400*, respectively), *EXP* = *Expansin* (*Solyc08g080060*), *XEG* = *Xyloglucan endotransglucosylase/hydrolase* (*Solyc11g040140*). Asterisks indicate a significant differential expression compared to the GFP samples (unpaired t-test, $p < 0.05$). NRQ = normalized relative quantities and transcript abundances are normalized against three tomato reference genes (*SlACT* (*Solyc03g078400*), *SlGAPDH* (*Solyc05g014470*) and *SlTUB* (*Solyc04g081490*)). Bars represent the mean, and the error bars indicate the standard error (+/- SE). Results are presented from three independent hairy root clones induced with 100 µM β-estradiol for 24 h.

In addition, several GO cellular component (GOCC) terms were enriched (cell wall, extracellular region, and plant-type cell wall), among which several cell wall-modifying enzymes (e.g., expansin, xyloglucan endotransglucosylase/hydrolase). Expression of enriched genes, as identified by RNA-seq, was validated by RT-qPCR (**Figure 4, B**). Among the tested genes (*Peroxidase* (*PRX*), *PRX24, PRX27, PRX57*, *Expansin* (*EXP*), *EXP-like*, and *Xyloglucan endotransglucosylase/hydrolase 5* (*XEG5*)), four were significantly differentially expressed in the *RipU-TurboID*-expressing hairy root samples compared to the *GFP-TurboID*-expressing samples (*PRX27, PRX57, EXP-like*, and *XEG5*).

Together, these results showed that *RipU* expression in tomato hairy root cultures induces specific transcriptional changes, among which significant differential expression of several oxidative stress-related genes.

DISCUSSION

PAMP recognition by pattern recognition receptors at the surface of plant cells activates PTI, an immune response involving the formation of intracellular immune signaling complexes and downstream defense responses. While nuclear signal transduction is steered by MAPKs to induce the expression of defense-related genes, ROS are induced and cell walls strengthened. As such,

pathogen T3Es frequently target these plant defense mechanisms to avoid their recognition. Upon translocation through the type III secretion system, effectors enter the host cell where they exert a wide array of functions. Many efforts have been taken to elucidate effector functioning, but information on *in planta* functioning of *Ralstonia* T3Es is mostly lacking[20]. Proteomics offers a powerful approach to elucidate protein function and biology. Proximity labeling in particular has enabled the identification of a protein's proximal partners – also referred to as the proxeome – in different models and different (subcellular) locations[31,32,34-36]. Multiple studies have reported the use of PL to investigate plant immunity[32,36,53], although, to our knowledge, only one reported study investigated root immunity[32]. Here, we used TurboID-mediated PL (referred to as TurboID-MS) to unravel the putative action of several RSSC core T3Es in tomato hairy root cultures, similar to a previous report that successfully used TurboID-MS to identify interaction partners of the *A. rhizogenes* RolB protein[32]. We here adopted the same approach to identify the putative proximal protein network of the core *Ralstonia* T3Es RipAJ, RipB, RipD, RipH1, RipH3 and RipU.

Although proximal targets were identified for RipB, RipD and RipU, few to no targets were identified for the RipAJ, RipH1 and RipH3 (**Figure 5**). Possible reasons might be technical such as steric hinderance of the C-terminal TurboID tag, the dynamic aspect of the interaction, limited expression/stability of the fusion protein (in our case, however, stable expression could be detected by means of immunoblotting), timepoint of sampling, or inaccessibility of lysine residues for TurboID-mediated biotinylation, among others[54]. It is also possible that (some of) these effectors function independently of protein interactors (e.g., enzymatic functions). Hence, the absence of a large proxeome does not mean that these effector are not relevant for disease establishment. Indeed, RipH1 and RipH3, together with RipH2, were shown to be collectively required for virulence in tomato[42]. The few tomato proteins found in the proxeome might thus still be relevant as, for RipH3, the disease resistance RPP8-like protein was found enriched, a protein related to plant immunity as it is induced by salicylic acid treatment or by pathogens such as

Peronospora parasitica responsible for downy mildew[55]. The alkaline/neutral invertase involved in the conversion of sucrose into fructose and glucose, which was identified as the sole potential interactor of RipAJ, might hint at a role of RipAJ in altering sugar levels for the suppression of plant immune responses or the enhancement of host susceptibility, as sucrose stimulates the production of secondary metabolites during defenses and represses sucrose non-fermenting-1-related kinase involved in sugar metabolism in stress conditions, and as sucrose transporters are primary causes for the formation of a carbohydrate-consuming sink tissue[56-59]. Further validation and research, however, is needed to support these hypotheses.

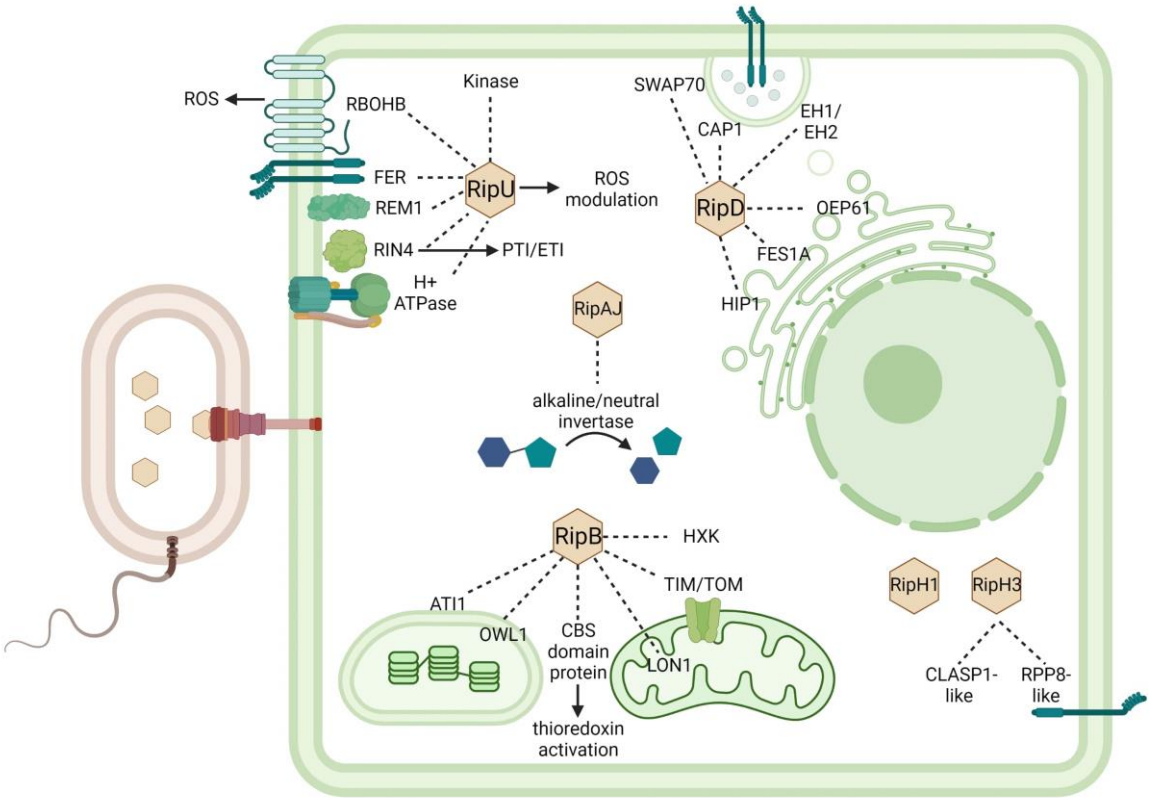

Figure 5. *R. pseudosolanacearum* type III effectors target different host pathways for establishing virulence and host susceptibility. Schematic overview of the interactomics results obtained in this work. The Arabidopsis homologs of the identified tomato root proteins are represented. Upon infection, T3Es are translocated into the plant cell for carrying out a diverse range of actions. RipU targets kinases and a RIN4-containing microdomain protein, while expression of oxidative stress-related genes is altered upon *RipU* expression. RipD targets the endomembrane system and RipB targets plastid proteins, as well as hexokinases (HXK) and CBS-domain

containing proteins. Alkaline/neutral invertase (converting sucrose into fructose and glucose) was identified as a putative proximal partner of RipAJ, and the CLASP1-like and RPP8-like proteins as proximal partners of RipH3. No significantly enriched proteins were identified for RipH1. Dotted lines indicate proximal protein partnering, as identified by TurboID-MS. This figure was created with BioRender.com.

For the T3Es RipB, RipD and RipU, several proximal proteins were identified. The core T3E RipB displays a nucleoside hydrolase domain, similar to the homologous *X. campestris* pv. *vesicatoria* XopQ (94% sequence identity) and *Pseudomonas syringae* pv. *tomato* HopQ1-1 (61% sequence identity)[60]. In tobacco, all three XopQ homologs are recognized by the NB-LRR immune receptor recognition of XopQ1 (Roq1), and are therefore considered ETI-triggering effectors in this host[61,62]. In tomato, however, no Roq1 homolog has been reported, and XopQ and HopQ1-1 have been reported to interact with 14-3-3 isoforms functioning in signal transduction during PTI and ETI, suggesting a virulence function in tomato[63-65]. Although 14-3-3 isoforms could not be detected in our analysis, potentially due to (one of) the abovementioned limitations of the method, mitochondrial and chloroplast proteins were identified as proximal partners. Further subcellular localization experiments of RipB in tomato roots might shed more light onto this hypothesis. A function directly related to the RipB nucleoside hydrolase domain, however, was less apparent, and could also not yet be demonstrated for its homologs HopQ1-1 and XopQ, as no activity for standard nucleoside substrates (e.g., inosine, guanosine, thymidine, cytidine and uridine) was identified[66,67]. However, RipB might bind to CBS-domain containing proteins, of which two were found enriched in the proxeome of RipB, to alter the level of (some of) the CBS target molecules such as AMP, S-AdoMet or inosine-5'-monophosphate. CBS-domain containing proteins can potentially target different types of thioredoxins in the chloroplast and mitochondria[68], which might explain the identification of both chloroplast and mitochondrial proximal proteins in our analysis. Overexpression of the gene encoding the CBS-domain-containing protein CBSX1 in *Arabidopsis* results in defective secondary wall thickening due to the activation of thioredoxins and

ROS scavenger proteins[68]. H-type thioredoxins are known targets of *Ralstonia* T3Es, as RipAY targets these redox regulators to suppress immune responses[27]. Hence, RipB might also target this pathway through interaction with CBS-domain-containing proteins and modification of its target molecules. Nevertheless, a different function for RipB can be hypothesized based on other enriched proteins such as the identification of several hexokinase (HXK) proteins (HXK1 and HXK3), mitochondrial proteins (the inner and outer mitochondrial transport proteins TIM and TOM; LON PROTEASE 1; ELONGATED MITOCHONDRIA 1; and ALTERED INHERITANCE OF MITOCHONDRIA PROTEIN 32-LIKE) and chloroplast proteins (ORIENTATION UNDER VERY LOW FLUENCES OF LIGHT 1; ATG8-INTERACTING PROTEIN 1) as proximal RipB partners (**Figure 5**). RipB might thus alter general plastid processes to interfere with, for example, ROS or energy production during biotic stress, although further investigation is needed. Subcellular localization studies and ROS assays could further validate these hypotheses.

The endomembrane system, comprising different cellular compartments such as the nuclear envelope, endoplasmic reticulum (ER), golgi apparatus and vesicles, spans the entire cell and is essential for modifying, packaging and transporting various lipids, metabolites and proteins. In response to pathogen infection, this system becomes crucial for the transport of immunity-related proteins and antimicrobial compounds to and from the PM. It therefore also holds hotspot targets for virulence factors such as T3Es. Besides the reported activities of tens of T3Es from phytopathogens such as *Xanthomonas* spp. or *P. syringae* acting on different parts of the endomembrane system, so far, only for the *Ralstonia* T3E RipD, a putative role in targeting the endomembrane system has been reported. More specifically, using Y2H screening, RipD was found to interact with *Arabidopsis* PRENYLATED RAB ACCEPTOR PROTEIN 1 (PRA1), a protein involved in ER-trafficking and protein transport from the Golgi[25]. Interestingly, in this Y2H screen, two directly interacting Arabidopsis PRA1 proteins (PRA1-F2 (*At1g55190*) and PRA1-F3 (*At3g13720*)) were both found to interact with RipD as well as with other effectors (RipA4, RipG6, and the *Golovinomyces*

orontii effector OEC65)[25,69]. In addition, the Y2H screen revealed interaction of PRA1-F2 with RipA1, suggesting a common effector target function for PRA1 proteins[25,69]. Tobacco localization studies also indicate RipD localization to the ER and to peroxisomes[70,71]. In line with this, in the tomato hairy root cultures expressing *RipD-TurboID*, many proteins involved in cellular trafficking were identified in our analysis (**Figure 5**). Besides the multiple proteins involved in the endomembrane system, clathrin-associated protein 1, EH-domain-containing protein 1 (EH1) and EH2, three components of the TPLATE complex, were found (**Figure 5**). EH1 and EH2 in particular localize to the PM and drive autophagosome formation at the ER-PM contact sites[72]. Autophagosome formation also requires the actin-binding protein SWAP70 that was identified in our analysis as well. Several proteins related to Hsp70 binding were enriched for RipD, such as one of the Arabidopsis ortholog of the human Hsp70-binding protein 1 FES1A, as well as the HSP70-INTERACTING PROTEIN 1 and the OUTER ENVELOPE PROTEIN 61, mediating Hsp70-dependent protein targeting to chloroplasts (**Figure 5**). Hsp70 proteins facilitate protein folding in stress conditions and protein translocation across the membrane, into the ER or other plant compartments such as chloroplasts and mitochondria[73,74]. Although not yet shown in plants, Hsp70 proteins have been shown to function in chaperone-mediated autophagy[75]. Considering that the *P. syringae* T3E HopI1 directly binds Hsp70 proteins, thereby recruiting Hsp70 to the chloroplasts, and that plants with depleted Hsp70-1 levels are more susceptible to *P. syringae* infection, it is possible that RipD somehow interferes with Hsp70 functioning to facilitate infection[76]. Together, our TurboID-MS results suggest a function for RipD in vesicle formation or trafficking, perhaps by internalization of PM-localized immune receptors or disruption of Hsp70 functions. Subcellular co-localization studies with endomembrane marker proteins could further strengthen this hypothesis.

The Rps GMI1000 T3E RipU has been shown to reduce the ROS burst and callose deposition when translocated by an effectorless *P. syringae* mutant to tobacco leaves, indicating that this

effector somehow interferes with the PTI response[4]. In agreement, RipU was shown to induce gene expression of *MAPKKKα*, *MKK2* and *SA-INDUCED PROTEIN KINASE* in tobacco, encoding important MAPK components connecting the perception of danger with the activation of the immunity response[4]. Although no tomato homologs from these genes were identified in our proteomic and transcriptomic analyses, intriguingly, the RipU proxeome that we identified consists of many components known to be involved in plant immunity in Arabidopsis[12,13,77]. More specifically, PTI-related proteins such as the FERONIA receptor, the guardee RIN4, REMORIN 1, H^+-ATPases AHA11 and AHA2, protein kinases, and RBOHB, among others, were enriched for RipU (**Figure 5**), many of which are also required for the ETI response[78-80]. The identified PTI and ETI immune complexes are tightly interconnected, as REMORIN 1 is known to form microdomains at the PM, where it recruits kinases and has been shown to interact with RIN4 and RBOHs[51,80], while RIN4 additionally interacts with H^+-ATPases[12]. The multiple kinases identified might thus also play a role in the immune response. Our results show that the immune complex, of which the components have been mainly identified in Arabidopsis, is also active in tomato root cells.

Remorin proteins, RIN4, H^+-ATPases and RBOHs are all also known targets of pathogen effectors, predominantly identified in leaf tissue[79,81-83]. Hence, the RipU proxeome thus reveals how RipU might cause the described suppression of the ROS burst[4]. Additionally, our transcriptomics analysis indicates that *RipU* expression causes significant changes in the oxidative stress response, among which upregulation of peroxidases involved in detoxification processes, and cell wall-modifying enzymes, further providing insight into how RipU might dampen the PTI and ETI responses via ROS level modulation and cell wall modification[4]. The many kinases identified in the proxeome might further hint towards ROS level modulation by RipU via interaction with kinase domains of several immune proteins. ROS assays, co-localization and co-immunoprecipitation studies could further substantiate these hypotheses.

CONCLUSION

Although further validation studies are required, our results show that the selected Rps GMI1000 core T3Es act at different (sub)cellular locations in tomato roots, likely for collective immune suppression and establishment of host susceptibility. Based on the results from our TurboID-MS analysis, RipB might target mitochondrial and chloroplast proteins to presumably alter the plant's redox status, RipD the plant's endomembrane system to potentially interfere with vesicle formation or transport, and RipU a RIN4-containing microdomain to presumably interfere with PTI/ETI responses via modulation of the ROS pathway. While most of our understanding of the immune regulator RIN4, and plant immunity in general, comes from studies performed in leaf tissues, we here shed light onto root immunity pathways, showing that RIN4 represents a likely target of root pathogens as well. We additionally show the potential of an innovative proteomics method (TurboID-based PL) for the functional characterization of effectors, information that is desperately needed in order to understand the pathogen's infection strategy.

ASSOCIATED CONTENT

Data Availability Statement

The mass spectrometry proteomics data have been deposited to the ProteomeXchange Consortium via the PRIDE partner repository[84] with the dataset identifier PXD048522.

Supporting Information

The Supporting Information is available free of charge at ACS website http://pubs.acs.org

Table S1. Primer sequences used in this study; Table S2. Significantly enriched protein targets of Rps GMI1000 T3Es identified by TurboID-MS in tomato hairy root cultures; Table S2b. Table S2. Significantly enriched protein targets of Rps GMI1000 T3Es identified by TurboID-MS in tomato hairy root cultures; Table S3. 1D enrichment annotations of the enriched proteins

identified in TurboID-MS in tomato hairy root cultures expressing Ralstonia T3Es; Table S4. Significantly differentially expressed genes for RipU identified in an RNA-seq analysis in tomato hairy root cultures; Table S5a. Pearson correlation between the different T3E-TurboID setups for TurboID-based proximity labeling; Table S5b. PCA analysis of the different T3E-TurboID setups for TurboID-based proximity labeling; Table S5c. Hierarchical clustering of the different T3E-TurboID setups for TurboID-based proximity labeling; Table S5d. Hierarchical clustering of the different T3E-TurboID setups for TurboID-based proximity labeling with imputation removed. Figure S1. Immunoblot analysis of tomato hairy root clones expressing Rps GMI1000 T3E-TurboID fusion proteins; Figure S2. Proximity-dependent biotin identification (TurbolD) enables the discovery of *Ralstonia* effector proximal partners in tomato.; Figure S3. Multiple sequence alignment of A0A3Q7H0Y2 and A0A3Q7H652, both identified by TurboID-MS, and Arabidopsis plasma membrane H^+-ATPases; Figure S4. Multiple sequence alignment of RIN4 amino acid sequences; Figure S5. Multiple sequence alignment of A0A3Q7FU72 identified by TurboID-MS and RBOHs; Figure S6. Shotgun proteomic analysis of the different T3E-TurboID setups; Figure S7. RipU co-localizes with RIN4.1, full-length (FL) A0A3Q7JBM6 and A0A3Q7JBM6 kinase domain in *N. benthamiana*.

AUTHOR INFORMATION

Author Contributions

J.D.R., J.V.V., S.G., N.P. and P.V.D. conceptualized the research. J.D.R., V.J., J.D., B.D.P., J.V.V., S.G. and P.V.D. supervised the experiments. J.D.R. and V.J. performed the experiments. Data analysis was performed by J.D.R. and P.V.D. Writing, review & editing was performed by J.D.R., S.G. and P.V.D. All authors contributed to reviewing and finalizing the manuscript text and gave approval to the final version of the manuscript.

Notes

The authors declare that the research was conducted in the absence of any commercial or financial relationships that could be construed as a potential conflict of interest.

ACKNOWLEDGMENTS

This work was supported by the European Research Council (ERC) under the European Union's Horizon 2020 research and innovation program (PROPHECY grant agreement No 803972), by the Research Foundation—Flanders (project number G.0511.20N to P.V.D. and Strategic Basic Research fellowship no. 1S83919N to J.D.R.) and by the Special Research Fund – Concerted Research Actions (project number BOF18-GOA-013 to S.G.). We thank the VIB proteomics core for their help with the MS-analyses, and Lieven Sterck for support with the RNA-seq analysis. We thank Annick Bleys for her help in preparing the manuscript.

ABBREVIATIONS

ACC	Acetyl-CoA carboxylase
AHA	AUTOINHIBITED H^+-ATPASE
BioID	Biotinylase-catalyzed proximity labeling
CaMV35S	Cauliflower mosaic virus 35S
CBS	Cystathione β-synthase
EH1	EH-DOMAIN CONTAINING PROTEIN 1
ER	Endoplasmic reticulum
ETI	Effector-triggered immunity
EXP	EXPANSIN
FL	Full-length
GFP	Green fluorescent protein

GO	Gene ontology
HXK	Hexokinase
LFQ	Label-free quantification
LRR	Leucine-rich repeat
MAMP	Microbial-associated molecular pattern
MAPK	Mitogen-activated protein kinase
NB	Nucleotide-binding
PAMP	Pathogen-associated microbial pattern
PL	Proximity labeling
PM	Plasma membrane
PPI	Protein–protein interaction
PRR	Pattern recognition receptors
PRX	PEROXIDASE
PTI	PAMP-triggered immunity
R	Resistance
RBOH	RESPIRATORY BURST OXIDASE HOMOLOG
RIN4	RPM1-INTERACTING PROTEIN 4
Ri	Root-inducing
Roq1	Recognition of XopQ1
ROS	Reactive oxygen species
RPM1	RESISTANCE TO PSEUDOMONAS SYRINGAE PV MACULICOLA 1
RPP8	RECOGNITION OF PERONOSPORA PARASITICA
RPS2	RESISTANT TO PSEUDOMONAS SYRINGAE 2
RSSC	*Ralstonia solanacearum* species complex
T3E	Type III effector
XEG	XYLOGLUCAN ENDOTRANSGLUCOSYLASE/HYDROLASE

Y2H Yeast 2-hybrid

REFERENCES

(1) Peeters, N.; Carrère, S.; Anisimova, M.; Plener, L.; Cazalé, A.-C.; Genin, S. Repertoire, unified nomenclature and evolution of the Type III effector gene set in the Ralstonia solanacearum species complex. *BMC Genomics* **2013**, *14* (1), 859.

(2) Sabbagh, C. R. R.; Carrere, S.; Lonjon, F.; et al. Pangenomic type III effector database of the plant pathogenic *Ralstonia* spp. *PeerJ* **2019**, *7*, e7346.

(3) Nakano, M.; Mukaihara, T. The type III effector RipB from *Ralstonia solanacearum* RS1000 acts as a major avirulence factor in *Nicotiana benthamiana* and other *Nicotiana* species. *Mol. Plant Pathol.* **2019**, *20* (9), 1237-1251.

(4) Cong, S.; Li, J.-Z.; Xiong, Z.-Z.; Wei, H.-L. Diverse interactions of five core type III effectors from *Ralstonia solanacearum* with plants. *J Genet Genomics* **2023**, *50* (5), 341-352.

(5) Nguyen, Q.-M.; Iswanto, A. B. B.; Son, G. H.; Kim, S. H. Recent advances in effector-triggered immunity in plants: new pieces in the puzzle create a different paradigm. *Int. J. Mol. Sci.* **2021**, *22* (9), 4709.

(6) Narusaka, M.; Kubo, Y.; Hatakeyama, K.; et al. Interfamily transfer of dual NB-LRR genes confers resistance to multiple pathogens. *PLoS ONE* **2013**, *8* (2), e55954.

(7) van der Hoorn, R. A. L.; Kamoun, S. From guard to decoy: A new model for perception of plant pathogen effectors. *Plant Cell* **2008**, *20* (8), 2009–2017.

(8) Axtell, M. J.; Staskawicz, B. J. Initiation of *RPS2*-specified disease resistance in *Arabidopsis* is coupled to the AvrRpt2-directed elimination of RIN4. *Cell* **2003**, *112* (3), 369-377.

(9) Mackey, D.; Belkhadir, Y.; Alonso, J. M.; Ecker, J. R.; Dangl, J. L. *Arabidopsis* RIN4 is a target of the type III virulence effector AvrRpt2 and modulates RPS2-mediated resistance. *Cell* **2003**, *112* (3), 379-389.

(10) Wilton, M.; Subramaniam, R.; Elmore, J.; Felsensteiner, C.; Coaker, G.; Desveaux, D. The type III effector HopF2$_{Pto}$ targets *Arabidopsis* RIN4 protein to promote *Pseudomonas syringae* virulence. *Proc. Natl. Acad. Sci. USA* **2010**, *107* (5), 2349-2354.

(11) Chung, E.-H.; El-Kasmi, F.; He, Y.; Loehr, A.; Dangl, J. L. A plant phosphoswitch platform repeatedly targeted by type III effector proteins regulates the output of both tiers of plant immune receptors. *Cell Host Microbe* **2014**, *16* (4), 484-494.

(12) Liu, J.; Elmore, J. M.; Fuglsang, A. T.; Palmgren, M. G.; Staskawicz, B. J.; Coaker, G. RIN4 functions with plasma membrane H^+-ATPases to regulate stomatal apertures during pathogen attack. *PLoS Biol.* **2009**, *7* (6), e1000139.

(13) Ray, S. K.; Macoy, D. M.; Kim, W.-Y.; Lee, S. Y.; Kim, M. G. Role of RIN4 in regulating PAMP-triggered immunity and effector-triggered immunity: current status and future perspectives. *Mol. Cells* **2019**, *42* (7), 503-511.

(14) Liu, J.; Elmore, J. M.; Lin, Z.-J. D.; Coaker, G. A receptor-like cytoplasmic kinase phosphorylates the host target RIN4, leading to the activation of a plant innate immune receptor. *Cell Host Microbe* **2011**, *9* (2), 137-146.

(15) Xu, N.; Luo, X.; Li, W.; Wang, Z.; Liu, J. The bacterial effector AvrB-induced RIN4 hyperphosphorylation is mediated by a receptor-like cytoplasmic kinase complex in *Arabidopsis*. *Mol. Plant-Microbe Interact.* **2017**, *30* (6), 502-512.

(16) Luo, Y.; Caldwell, K. S.; Wroblewski, T.; Wright, M. E.; Michelmore, R. W. Proteolysis of a negative regulator of innate immunity is dependent on resistance genes in tomato and *Nicotiana benthamiana* and induced by multiple bacterial effectors. *Plant Cell* **2009**, *21* (8), 2458-2472.

(17) Jelenska, J.; Lee, J.; Manning, A. J.; et al. *Pseudomonas syringae* effector HopZ3 suppresses the bacterial AvrPto1-tomato PTO immune complex via acetylation. *PLoS Pathog.* **2021**, *17* (11), e1010017.
(18) Lang, J.; Genot, B.; Bigeard, J.; Colcombet, J. MPK3 and MPK6 control salicylic acid signaling by up-regulating *NLR* receptors during pattern-and effector-triggered immunity. *J. Exp. Bot.* **2022**, *73* (7), 2190-2205.
(19) De Coninck, B.; Timmermans, P.; Vos, C.; Cammue, B. P.; Kazan, K. What lies beneath: belowground defense strategies in plants. *Trends Plant Sci.* **2015**, *20* (2), 91-101.
(20) De Ryck, J.; Van Damme, P.; Goormachtig, S. From prediction to function: Current practices and challenges towards the functional characterization of type III effectors. *Front. Microbiol.* **2023**, *14*, 1113442.
(21) Bontinck, M.; Van Leene, J.; Gadeyne, A.; et al. Recent trends in plant protein complex analysis in a developmental context. *Front. Plant Sci.* **2018**, *9*, 640.
(22) De Meyer, M.; De Ryck, J.; Goormachtig, S.; Van Damme, P. Keeping in touch with type-III secretion system effectors: mass spectrometry-based proteomics to study effector–host protein–protein interactions. *Int. J. Mol. Sci.* **2020**, *21* (18), 6891.
(23) Erffelinck, M.-L.; Ribeiro, B.; Perassolo, M.; et al. A user-friendly platform for yeast two-hybrid library screening using next generation sequencing. *PLoS ONE* **2018**, *13* (12), e0201270.
(24) Gingras, A.-C.; Abe, K. T.; Raught, B. Getting to know the neighborhood: using proximity-dependent biotinylation to characterize protein complexes and map organelles. *Curr. Opin. Chem. Biol.* **2019**, *48*, 44-54.
(25) González-Fuente, M.; Carrère, S.; Monachello, D.; et al. EffectorK, a comprehensive resource to mine for *Ralstonia*, *Xanthomonas*, and other published effector interactors in the *Arabidopsis* proteome. *Mol. Plant Pathol.* **2020**, *21* (10), 1257-1270.
(26) Qi, P.; Huang, M.; Hu, X.; et al. A *Ralstonia solanacearum* effector targets TGA transcription factors to subvert salicylic acid signaling. *Plant Cell* **2022**, *34* (5), 1666-1683.
(27) Sang, Y.; Wang, Y.; Ni, H.; et al. The *Ralstonia solanacearum* type III effector RipAY targets plant redox regulators to suppress immune responses. *Mol. Plant Pathol.* **2018**, *19* (1), 129-142.
(28) Sun, Y.; Li, P.; Deng, M.; et al. The *Ralstonia solanacearum* effector RipAK suppresses plant hypersensitive response by inhibiting the activity of host catalases. *Cell. Microbiol.* **2017**, *19* (8), e12736.
(29) Xian, L.; Yu, G.; Wei, Y.; et al. A bacterial effector protein hijacks plant metabolism to support pathogen nutrition. *Cell Host Microbe* **2020**, *28* (4), 548-557.
(30) Yu, G.; Xian, L.; Xue, H.; et al. A bacterial effector protein prevents MAPK-mediated phosphorylation of SGT1 to suppress plant immunity. *PLoS Pathog.* **2020**, *16* (9), 1008933.
(31) Arora, D.; Abel, N. B.; Liu, C.; et al. Establishment of proximity-dependent biotinylation approaches in different plant model systems. *Plant Cell* **2020**, *32* (11), 3388-3407.
(32) Gryffroy, L.; Ceulemans, E.; Manosalva Pérez, N.; et al. Rhizogenic *Agrobacterium* protein RolB interacts with the TOPLESS repressor proteins to reprogram plant immunity and development. *Proc. Natl. Acad. Sci. USA* **2023**, *120* (3), e2210300120.
(33) Gryffroy, L.; De Ryck, J.; Jonckheere, V.; Goormachtig, S.; Goossens, A.; Van Damme, P. Cataloguing protein complexes *in planta* using turboID-catalyzed proximity labeling. *Methods Mol. Biol.* **2023**, *2690*, 311-334.
(34) Kim, T.-W.; Park, C. H.; Hsu, C.-C.; et al. Application of TurboID-mediated proximity labeling for mapping a GSK3 kinase signaling network in Arabidopsis. *bioRxiv* **2019**, *636324*.
(35) Mair, A.; Xu, S.-L.; Branon, T. C.; Ting, A. Y.; Bergmann, D. C. Proximity labeling of protein complexes and cell-type-specific organellar proteomes in *Arabidopsis* enabled by TurboID. *eLife* **2019**, *8*, e47864.
(36) Zhang, Y.; Song, G.; Lal, N. K.; et al. TurboID-based proximity labeling reveals that UBR7 is a regulator of N NLR immune receptor-mediated immunity. *Nat. Commun.* **2019**, *10* (1), 3252.

(37) Ron, M.; Kajala, K.; Pauluzzi, G.; et al. Hairy root transformation using *Agrobacterium rhizogenes* as a tool for exploring cell type-specific gene expression and function using tomato as a model. *Plant Physiol.* **2014**, *166* (2), 455-469.
(38) Van Leene, J.; Stals, H.; Eeckhout, D.; et al. A tandem affinity purification-based technology platform to study the cell cycle interactome in *Arabidopsis thaliana*. *Mol. Cell. Proteomics* **2007**, *6* (7), 1226-1238.
(39) Zuo, J.; Niu, Q.-W.; Chua, N.-H. An estrogen receptor-based transactivator XVE mediates highly inducible gene expression in transgenic plants. *Plant J.* **2000**, *24* (2), 265-273.
(40) Patro, R.; Duggal, G.; Love, M. I.; Irizarry, R. A.; Kingsford, C. Salmon provides fast and bias-aware quantification of transcript expression. *Nat. Methods* **2017**, *14* (4), 417-419.
(41) Van Bel, M.; Silvestri, F.; Weitz, E. M.; et al. PLAZA 5.0: extending the scope and power of comparative and functional genomics in plants. *Nucleic Acids Res.* **2022**, *50* (D1), D1468-D1474.
(42) Chen, L.; Shirota, M.; Zhang, Y.; Kiba, A.; Hikichi, Y.; Ohnishi, K. Involvement of HLK effectors in *Ralstonia solanacearum* disease development in tomato. *Journal of general plant pathology* **2014**, *80*, 79-84.
(43) Pensec, F.; Lebeau, A.; Daunay, M.-C.; Chiroleu, F.; Guidot, A.; Wicker, E. Towards the identification of type III effectors associated with *Ralstonia solanacearum* virulence on tomato and eggplant. *Phytopathology* **2015**, *105* (12), 1529-1544.
(44) Cox, J.; Hein, M. Y.; Luber, C. A.; Paron, I.; Nagaraj, N.; Mann, M. Accurate proteome-wide label-free quantification by delayed normalization and maximal peptide ratio extraction, termed MaxLFQ. *Mol. Cell. Proteomics* **2014**, *13* (9), 2513-2526.
(45) Cox, J.; Mann, M. 1D and 2D annotation enrichment: a statistical method integrating quantitative proteomics with complementary high-throughput data. *BMC Bioinformatics* **2012**, *13 Suppl 16* (Suppl 16), S12.
(46) Tyanova, S.; Temu, T.; Cox, J. The MaxQuant computational platform for mass spectrometry-based shotgun proteomics. *Nat. Protoc.* **2016**, *11* (12), 2301-2319.
(47) Haruta, M.; Sabat, G.; Stecker, K.; Minkoff, B. B.; Sussman, M. R. A peptide hormone and its receptor protein kinase regulate plant cell expansion. *Science* **2014**, *343* (6169), 408-411.
(48) Haruta, M.; Tan, L. X.; Bushey, D. B.; Swanson, S. J.; Sussman, M. R. Environmental and genetic factors regulating localization of the plant plasma membrane H^+-ATPase. *Plant Physiol.* **2018**, *176* (1), 364-377.
(49) Kessler, S. A.; Shimosato-Asano, H.; Keinath, N. F.; et al. Conserved molecular components for pollen tube reception and fungal invasion. *Science* **2010**, *330* (6006), 968-971.
(50) Ji, D.; Liu, W.; Cui, X.; et al. A receptor-like kinase SlFERL mediates immune responses of tomato to *Botrytis cinerea* by recognizing BcPG1 and fine-tuning MAPK signaling. *New Phytol.* **2023**, *240* (3), 1189-1201.
(51) Cai, J.; Chen, T.; Wang, Y.; Qin, G.; Tian, S. SlREM1 triggers cell death by activating an oxidative burst and other regulators. *Plant Physiol.* **2020**, *183* (2), 717-732.
(52) Gardiner, J.; Overall, R.; Marc, J. PDZ domain proteins: 'Dark matter'of the plan proteome? *Mol. Plant* **2011**, *4* (6), 933-937.
(53) Khan, M.; Youn, J.-Y.; Gingras, A.-C.; Subramaniam, R.; Desveaux, D. *In planta* proximity dependent biotin identification (BioID). *Sci. Rep.* **2018**, *8* (1), 9212.
(54) do Nascimento Moreira, C. M.; Kelemen, C. D.; Obado, S. O.; et al. Impact of inherent biases built into proteomic techniques: proximity labeling and affinity capture compared. *J. Biol. Chem.* **2023**, *299* (1), 102726.
(55) Mohr, T. J.; Mammarella, N. D.; Hoff, T.; Woffenden, B. J.; Jelesko, J. G.; McDowell, J. M. The *Arabidopsis* downy mildew resistance gene *RPP8* is induced by pathogens and salicylic acid and is regulated by W box *cis* elements. *Mol. Plant-Microbe Interact.* **2010**, *23* (10), 1303-1315.
(56) Baena-González, E.; Rolland, F.; Thevelein, J. M.; Sheen, J. A central integrator of transcription networks in plant stress and energy signalling. *Nature* **2007**, *448* (7156), 938-942.

(57) Essmann, J.; Schmitz-Thom, I.; Schön, H.; Sonnewald, S.; Weis, E.; Scharte, J. RNA interference-mediated repression of cell wall invertase impairs defense in source leaves of tobacco. *Plant Physiol.* **2008**, *147* (3), 1288-1299.

(58) Liu, Y.-H.; Song, Y.-H.; Ruan, Y.-L. Sugar conundrum in plant–pathogen interactions: roles of invertase and sugar transporters depend on pathosystems. *J. Exp. Bot.* **2022**, *73* (7), 1910-1925.

(59) Morkunas, I.; Narożna, D.; Nowak, W.; Samardakiewicz, S.; Remlein-Starosta, D. Cross-talk interactions of sucrose and *Fusarium oxysporum* in the phenylpropanoid pathway and the accumulation and localization of flavonoids in embryo axes of yellow lupine. *J. Plant Physiol.* **2011**, *168* (5), 424-433.

(60) Gazi, A. D.; Kokkinidis, M.; Fadouloglou, V. E. α-Helices in the type III secretion effectors: A prevalent feature with versatile roles. *Int. J. Mol. Sci.* **2021**, *22* (11), 5412.

(61) Staskawicz, B. J.; Schultink, A. C. ROQ1 provides resistance to both xanthomonas and pseudomonas in plants. (2019).

(62) Thomas, N. C.; Hendrich, C. G.; Gill, U. S.; Allen, C.; Hutton, S. F.; Schultink, A. The immune receptor Roq1 confers resistance to the bacterial pathogens *Xanthomonas*, *Pseudomonas syringae*, and *Ralstonia* in tomato. *Front. Plant Sci.* **2020**, *11*, 463.

(63) Giska, F.; Lichocka, M.; Piechocki, M.; et al. Phosphorylation of HopQ1, a type III effector from *Pseudomonas syringae*, creates a binding site for host 14-3-3 proteins. *Plant Physiol.* **2013**, *161* (4), 2049-2061.

(64) Li, W.; Yadeta, K. A.; Elmore, J. M.; Coaker, G. The *Pseudomonas syringae* effector HopQ1 promotes bacterial virulence and interacts with tomato 14-3-3 proteins in a phosphorylation-dependent manner. *Plant Physiol.* **2013**, *161* (4), 2062-2074.

(65) Teper, D.; Salomon, D.; Sunitha, S.; Kim, J. G.; Mudgett, M. B.; Sessa, G. *Xanthomonas euvesicatoria* type III effector X op Q interacts with tomato and pepper 14–3–3 isoforms to suppress effector-triggered immunity. *Plant J.* **2014**, *77* (2), 297-309.

(66) Gupta, M. K.; Nathawat, R.; Sinha, D.; Haque, A. S.; Sankaranarayanan, R.; Sonti, R. V. Mutations in the predicted active site of *Xanthomonas oryzae* pv. *oryzae* XopQ differentially affect virulence, suppression of host innate immunity, and induction of the HR in a nonhost plant. *Mol. Plant-Microbe Interact.* **2015**, *28* (2), 195-206.

(67) Li, W.; Chiang, Y.-H.; Coaker, G. The HopQ1 effector's nucleoside hydrolase-like domain is required for bacterial virulence in Arabidopsis and tomato, but not host recognition in tobacco. *PLoS ONE* **2013**, *8* (3), e59684.

(68) Yoo, K. S.; Ok, S. H.; Jeong, B. C.; et al. Single cystathionine β-synthase domain-containing proteins modulate development by regulating the thioredoxin system in *Arabidopsis*. *Plant Cell* **2011**, *23* (10), 3577-3594.

(69) Mukhtar, M. S.; Carvunis, A.-R.; Dreze, M.; et al. Independently evolved virulence effectors converge onto hubs in a plant immune system network. *Science* **2011**, *333* (6042), 596-601.

(70) Denne, N. L.; Hiles, R. R.; Kyrysyuk, O.; Iyer-Pascuzzi, A. S.; Mitra, R. M. *Ralstonia solanacearum* effectors localize to diverse organelles in *Solanum* hosts. *Phytopathology* **2021**, *111* (12), 2213-2226.

(71) Jeon, H.; Kim, W.; Kim, B.; et al. *Ralstonia solanacearum* type III effectors with predicted nuclear localization signal localize to various cell compartments and modulate immune responses in *Nicotiana* spp. *Plant Pathol. J.* **2020**, *36* (1), 43-53.

(72) Wang, P.; Pleskot, R.; Zang, J.; et al. Plant AtEH/Pan1 proteins drive autophagosome formation at ER-PM contact sites with actin and endocytic machinery. *Nat. Commun.* **2019**, *10*, 5132.

(73) Berka, M.; Kopecká, R.; Berková, V.; Brzobohatý, B.; Černý, M. Regulation of heat shock proteins 70 and their role in plant immunity. *J. Exp. Bot.* **2022**, *73* (7), 1894-1909.

(74) Schleiff, E.; Becker, T. Common ground for protein translocation: access control for mitochondria and chloroplasts. *Nat. Rev. Mol. Cell Biol.* **2011**, *12* (1), 48-59.

(75) Fernández-Fernández, M. R.; Gragera, M.; Ochoa-Ibarrola, L.; Quintana-Gallardo, L.; Valpuesta, J. M. Hsp70–a master regulator in protein degradation. *FEBS Lett.* **2017**, *591* (17), 2648-2660.

(76) Jelenska, J.; van Hal, J. A.; Greenberg, J. T. *Pseudomonas syringae* hijacks plant stress chaperone machinery for virulence. *Proc. Natl. Acad. Sci. USA* **2010**, *107* (29), 13177-13182.
(77) Ma, Z.; Sun, Y.; Zhu, X.; Yang, L.; Chen, X.; Miao, Y. Membrane nanodomains modulate formin condensation for actin remodeling in Arabidopsis innate immune responses. *Plant Cell* **2022**, *34* (1), 374-394.
(78) Hurley, B.; Subramaniam, R.; Guttman, D. S.; Desveaux, D. Proteomics of effector-triggered immunity (ETI) in plants. *Virulence* **2014**, *5* (7), 752-760.
(79) Li, X.; Zhang, H.; Tian, L.; et al. Tomato SlRbohB, a member of the NADPH oxidase family, is required for disease resistance against *Botrytis cinerea* and tolerance to drought stress. *Front. Plant Sci.* **2015**, *6*, 463.
(80) Liu, J.; Elmore, J. M.; Coaker, G. Investigating the functions of the RIN4 protein complex during plant innate immune responses. *Plant Signal. Behav.* **2009**, *4* (12), 1107-1110.
(81) Albers, P.; Üstün, S.; Witzel, K.; Kraner, M.; Börnke, F. A Remorin from *Nicotiana benthamiana* interacts with the *Pseudomonas* type-III effector protein HopZ1a and is phosphorylated by the immune-related kinase PBS1. *Mol. Plant-Microbe Interact.* **2019**, *32* (9), 1229-1242.
(82) Hurley, B.; Lee, D.; Mott, A.; et al. The *Pseudomonas syringae* type III effector HopF2 suppresses Arabidopsis stomatal immunity. *PLoS ONE* **2014**, *9* (12), e114921.
(83) Lee, D.; Bourdais, G.; Yu, G.; Robatzek, S.; Coaker, G. Phosphorylation of the plant immune regulator RPM1-INTERACTING PROTEIN4 enhances plant plasma membrane H^+-ATPase activity and inhibits flagellin-triggered immune responses in Arabidopsis. *Plant Cell* **2015**, *27* (7), 2042-2056.
(84) Perez-Riverol, Y.; Bai, J.; Bandla, C.; et al. The PRIDE database resources in 2022: a hub for mass spectrometry-based proteomics evidences. *Nucleic Acids Res.* **2022**, *50* (D1), D543-D552.

For TOC Only

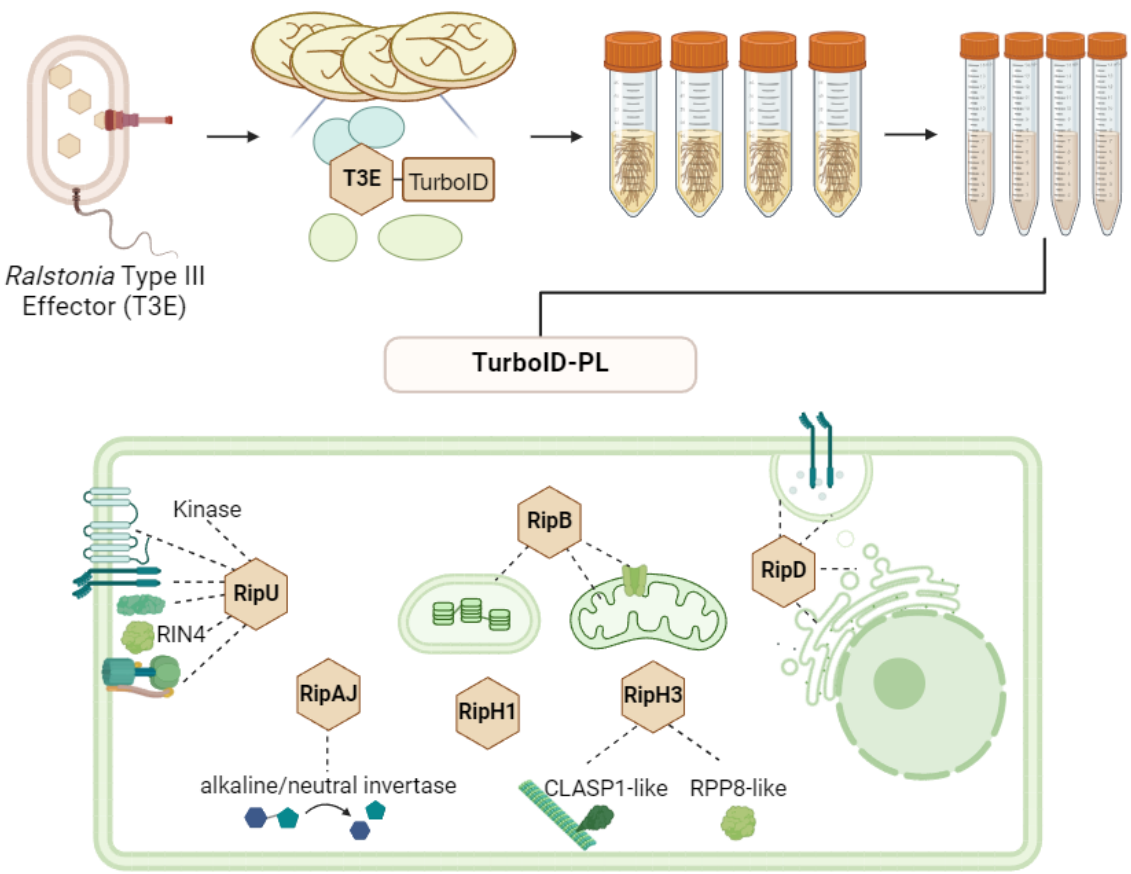
T3E
TurboID
Ralstonia Type III Effector (T3E)
TurboID-PL
Kinase
RipU
RIN4
RipB
RipD
RipAJ
RipH1
RipH3
alkaline/neutral invertase
CLASP1-like
RPP8-like